

1 **Report 3**

2 **Reply to Anonymous Referee #4**

3 **General comments:**

4 This manuscript presents the simultaneous retrieval of aerosol optical depth (AOD), single
5 scattering albedo (SSA) and directional-hemispheric reflectance (DHR) from the
6 Directional Polarimetric Camera (DPC) aboard China's Gaofen-5 satellite. The sensitivity
7 analysis, performance evaluation by synthetic data, and application to actual DPC data are
8 discussed. The sensitivity analysis demonstrates the challenges in retrieving SSA values
9 from the DPC data, while the algorithm based on optimal estimation is designed to
10 overcome the challenges. The performance of the developed algorithm is evaluated both
11 based on synthetic data and Aerosol Robotic Network (AERONET) data. A case study and
12 global maps are also presented. While this manuscript covers a very challenging topic and
13 takes a conservative approach, the restrained reproducibility and incomplete analysis limit
14 the value of this manuscript to the research community. The manuscript would require a
15 substantial revision for final publication in AMT if authors are willing to do so. The
16 following points should be addressed to increase the impact of this manuscript.

17 We appreciate the reviewer for the constructive comments and thoughtful suggestions,
18 which are very helpful in improving our manuscript. We have carefully considered all the
19 comments and revised the manuscript accordingly. Below is a detailed point-by-point
20 response to these comments.

- 21 1. Identifying the original dataset. This study uses DPC, MODIS, ERA5, HYCOM
22 and AERONET data. However, some descriptions are missing regarding product
23 type, time period (start date and end date), dataset size (number of pixels and
24 number of AERONET sites). Please detail as much as possible, and if not sufficient,
25 use Appendix to describe the data so that readers can collect necessary data.

26 Thanks for the suggestion. The temporal coverage of this study is primarily constrained by
27 the availability of DPC observations. Specifically, we have six months of DPC data,

28 encompassing April, July, and October 2019, as well as January–March 2020. The MODIS,
29 ERA5, HYCOM, and AERONET teams provide continuous data covering this period,
30 enabling the retrieval and validation in this study. We have added this information in the
31 manuscript in L75-77:

32 *Six months of DPC Level 1 data, encompassing April, July, and October 2019, as*
33 *well as January-March 2020, are used in the retrieval in this study. The AERONET,*
34 *MODIS, as well as other auxiliary data are selected from the same periods.*

35 The temporal and spatial resolution of the auxiliary data are described in Sect. 2.2 in the
36 manuscript. We have summarized them in Table 1 in the manuscript.

37 2. Describing applied corrections and filters. It appears that authors have applied some
38 corrections to DPC data, but the details are not presented. Some references are
39 provided, but it would be beneficial to briefly describe the outline of the applied
40 corrections. In addition, the “fine-mode filtering” of AERONET data (and
41 potentially retrieval results) remains unclear. Documenting the number of points
42 (pixels) before and after filtering would help readers understand the extent of
43 filtering.

44 Thanks for the suggestion. Following the launch of DPC, gradual aging of its optical
45 components led to a drift in radiometric response, with the magnitude of the drift related
46 to both time and VZA. Zhu et al. (2022) calibrated this drift using DPC observations over
47 deep ocean regions through the Rayleigh method and provided monthly VZA-dependent
48 calibration coefficients. In this study, DPC observations were corrected using these
49 calibration coefficients to reduce radiometric biases as much as possible. We have added
50 details about the calibration in the manuscript in L82-89:

51 *The radiometric response of DPC/GaoFen-5 is progressively drifting over time and*
52 *is related to VZA. Zhu et al. (2022) developed a method based on Rayleigh*
53 *scattering over the ocean to correct this drift. In deep ocean regions with very low*
54 *aerosol loading and low surface reflectance, the TOA radiance observed by*
55 *satellite sensors is dominated by atmospheric Rayleigh scattering, which can be*
56 *accurately simulated using radiative transfer models. By comparing simulated*

57 *radiances with DPC observations over such regions, Zhu et al. (2022) provided*
58 *monthly VZA-dependent calibration coefficients at 443, 490, 565, and 670 nm. The*
59 *calibration uncertainties are about 1-7 % (depending on the wavelength and VZA).*
60 *In this study, these Rayleigh scattering-based calibration coefficients are applied*
61 *to correct DPC's scalar reflectance at 443, 490, 565, and 670 nm.*

62 In this study, only the official AERONET Level 2.0 quality control criteria (excluding the
63 AOD threshold) were applied to the Level 1.5 inversion data to ensure the accuracy of
64 AERONET SSA. No additional screening was applied to AERONET observations.
65 However, quality control was performed on the retrieval results, based on whether the
66 retrieved parameters exceeded predefined thresholds. Retrievals yielding physically
67 unreasonable values outside these thresholds were regarded as failed cases and were
68 excluded from further analysis. The predefined thresholds have been summarized in Table
69 3 in the manuscript.

70 3. Clarifying the measurement vector, a priori state vector, model parameters, and
71 variance-covariance matrix in the retrieval algorithm. The developed algorithm is
72 based on optimal estimation. Optimal estimation is a blending of measurements and
73 a priori information based on variance, and therefore the information on the a priori
74 state vector, model parameters, and variance-covariance matrices should be
75 documented and the reasons behind the choice should be described. This
76 shortcoming makes the study non-reproducible and the interpretation of results very
77 challenging. In addition, the measurement vector elements remain ambiguous. It is
78 requested to document the used spectral channel, polarization or not, and the
79 filtering applied to the input data.

80 Thanks for this important suggestion. We agree that a clear and complete description of
81 the measurement vector, the a priori state vector, the model parameters, and the associated
82 variance-covariance matrices is essential. In the revised manuscript, we have expanded the
83 description of the retrieval algorithm, and added two tables (Tables 2 and 3) to summarize
84 these settings. Specifically, Table 2 summarizes the selected DPC measurements and their
85 associated uncertainty specifications, while Table 3 lists the prescribed a priori values and
86 uncertainties for aerosol and surface parameters.

87 In particular, we have clarified the composition of the measurement vector \mathbf{y} , including the
88 spectral channels, the use of polarization information, and the angular sampling strategy,
89 in L167-173:

90 *The measurement vector, \mathbf{y} , is constructed with calibrated scalar reflectance at 443,*
91 *490, 565, and 670, as well as DOLP at 490 and 670 nm from several angles...Pixels*
92 *with fewer than 9 viewing angles, which are primarily located near the scan edges,*
93 *were therefore excluded. For the remaining pixels, observations from the first 9*
94 *viewing angles were used in the retrieval to maintain a fixed number of viewing*
95 *angles for all pixels.*

96 The measurement error covariance matrix is calculated based on DPC calibration
97 uncertainties, which has also been specified in L176-178:

98 *Therefore, this study adopts the official pre-launch laboratory calibration errors,*
99 *namely 5 % radiance errors and 0.02 DOLP errors (Li et al., 2018), as the*
100 *observational errors used to construct the measurement error covariance matrix.*

101 In addition, the retrieval parameters composing the state vector \mathbf{x} and the model
102 parameterization used over land and water have been made explicit in L180-189:

103 *The state vector, \mathbf{x} , is composed of aerosol and surface parameters. Particularly,*
104 *for land surfaces, the state vector \mathbf{x} consists of AOD ($\tau(\lambda)$), SSA ($\omega(\lambda)$), kernel*
105 *intensity parameters of RTLS model ($K(\lambda)$, k_{vol} , and k_{geo} in Eq. 2), and the scale*
106 *factor of BPDF-NDVI model (C in Eq. 8)...For water surfaces, only $\tau(\lambda)$ and $\omega(\lambda)$*
107 *are retrieved as components of the state vector \mathbf{x} , and the New Cox-Munk model is*
108 *implemented to compute the surface reflectance (Spurr, 2006). The wavelength-*
109 *dependent parameters, $\tau(\lambda)$, $\omega(\lambda)$, and $K(\lambda)$, are retrieved at 443, 490, 565, and*
110 *670 nm, corresponding to the wavelengths at which DPC observations are used to*
111 *construct the measurement vector.*

112 The description of a priori values and the corresponding uncertainties has been clarified in
113 L189-192:

114 *For AOD and SSA, the a priori state vector and its associated error covariance*
115 *matrix are prescribed as fixed values, derived from the mean and variance of*
116 *AERONET measurements. The a priori estimates of surface properties are also*
117 *fixed, with their errors defined by the corresponding ranges of variability.*

118 Finally, we have stated that the cost function minimization is implemented through an
119 iterative Gauss–Newton approach (L201):

120 *The algorithm minimizes the cost function defined in Eq. 4 using an iterative*
121 *Gauss–Newton method to obtain the final retrieval results.*

122 We believe these revisions address the reviewer’s concerns by documenting the
123 measurement vector elements, the state vector and model parameterization, and the
124 variance-covariance assumptions and a priori settings, with configurations listed in Tables
125 2 and 3.

126 4. [Improving the compatibility with other studies.](#) The validation sections discuss
127 [mainly the results at 443 nm, but a number of previous research use 550 nm for](#)
128 [comparison. The contribution of fine-mode particles is substantially different](#)
129 [between two wavelengths and presented results are not directly comparable. Even](#)
130 [if the results at 550 nm may not be very encouraging, it serves the community to](#)
131 [understand what to improve in the next instrument and algorithm development.](#)

132 Thanks for the suggestion. The retrieval results of this study are primarily validated against
133 AERONET observations, which provide high-quality aerosol measurements and are
134 widely used as a reference dataset. Particularly, AERONET inversion products are
135 available at 440, 675, 870, and 1020 nm, thus an important consideration for focusing on
136 the 440 nm results is the direct availability of AERONET observations at this wavelength.
137 In the revised manuscript, we have added results at additional wavelengths and included
138 comparisons with other studies.

139 Other satellite products, such as the widely used MODIS AOD, mainly provide retrievals
140 at 550 nm and are commonly applied in large-scale or spatial pattern analysis. Accordingly,

141 maps of the retrieval results at 550 nm have been included in the Supplement and compared
142 with MODIS AOD.

143 5. Deepening the analysis of the case study and global statistics. Although authors
144 mention in the conclusions that the analysis remains qualitative, there are
145 unexplained patterns and characteristics in the case study and the global map.
146 Figure 9 seems to be influenced by the number of view directions (bands-like
147 patterns running in satellite cross-track direction) and Figures 10 and 11 show the
148 difficulties probably related to cloud mask (Southern Ocean AOT values) and view
149 geometry (sharp contrast of SSA that stretches along the orbit).

150 We thank the reviewer for the helpful comment.

151 (1) In this study, the number of viewing angles used in the retrieval are fixed. We
152 screened pixels with fewer than 9 viewing angles, and only use observations from
153 the first 9 viewing angles for the remaining pixels. We have added this detail in the
154 manuscript in L171-173:

155 *Pixels with fewer than 9 viewing angles, which are primarily located near the scan*
156 *edges, were therefore excluded. For the remaining pixels, observations from the*
157 *first 9 viewing angles were used in the retrieval to maintain a fixed number of*
158 *viewing angles for all pixels.*

159 Therefore, the band-like patterns in Figure 9 are probably not caused by the number multi-
160 angle observation itself. Instead, they might be related to variations in viewing-angle
161 distribution between successive cross-track scans of DPC.

162 As mentioned in the revised manuscript in L79:

163 *However, after launch, DPC exhibited a gradual change in radiometric sensitivity,*
164 *primarily due to aging of the optical components. This drift is dependent on both*
165 *wavelength and field of view and can introduce increasing systematic biases if not*
166 *properly corrected.*

167 Due to aging of the DPC optical components, the radiometric response experienced VZA-
168 dependent drift. When the satellite switches from one cross-track scan to the next, the

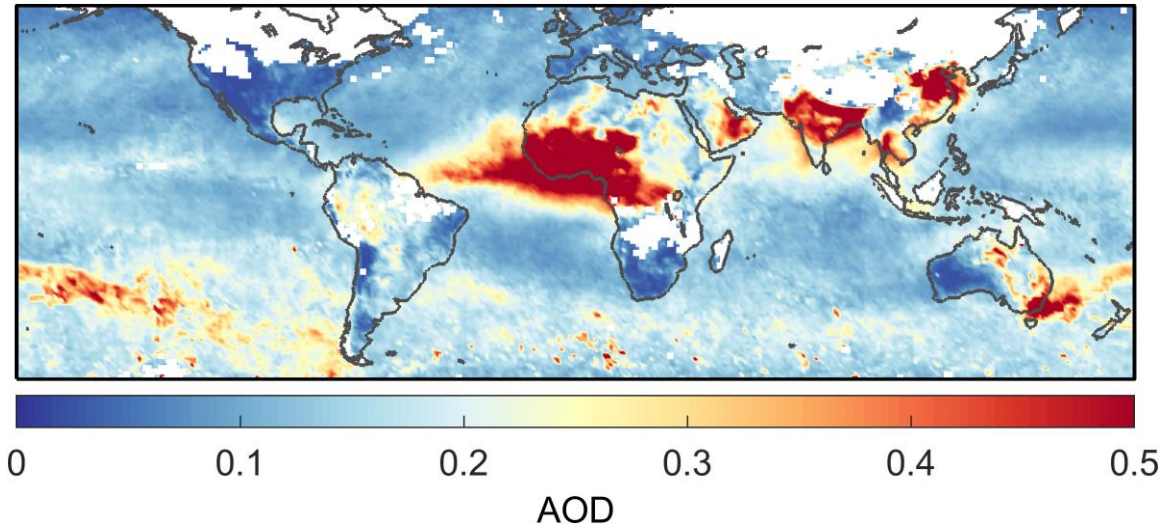
169 distribution of viewing angles changes sharply. As a result, the magnitude of radiometric
170 drift may differ between adjacent scans. Although radiometric calibration is applied before
171 the retrieval process, this correction cannot completely remove the VZA-dependent
172 residual errors. These residual differences may lead to meridional discontinuities in the
173 retrieval results.

174 We have revised the manuscript in L389-396 to clarify this explanation:

175 *The meridional discontinuities in Fig. 9(b,c) primarily originate from abrupt*
176 *changes in the observed radiance between successive cross-track scans of DPC,*
177 *rather than from the retrieval algorithm itself. These discontinuities arise when the*
178 *instrument switches from one cross-track scan to the next, during which the*
179 *distribution of viewing angle changes. Due to aging of the DPC optical components,*
180 *the radiometric response exhibits VZA-dependent drifts. Consequently, variations*
181 *in viewing-angle distribution lead to variations in the magnitude of this drift,*
182 *leading to radiance inconsistencies between adjacent scans. Although radiometric*
183 *calibration is applied prior to the retrieval, the VZA-dependent residual errors*
184 *cannot be completely eliminated. These residual radiometric differences ultimately*
185 *result in the meridional striping patterns seen in the retrieval results.*

186 (2) As for the abnormally high AOD values observed over the Southern Ocean in Fig.
187 10, we conducted further examinations using true-color imagery and MODIS AOD
188 products. The true-color imagery for early January 2020 reveals extensive smoke
189 plumes over the Southern Ocean originating from southeastern Australia and
190 gradually transported eastward. This indicates that large amounts of biomass-
191 burning aerosols were present over the region during this period. The MODIS
192 monthly AOD product for January 2020 also shows anomalously high AOD over
193 the Southern Ocean, with values exceeding 0.5 in some areas (Fig. R3-1). The
194 spatial pattern and magnitude are generally consistent with our retrieval results.
195 Thus, this magnitude is likely reasonable. We have added the corresponding
196 MODIS AOD map to the Supplement material, and included a relevant discussion
197 in the manuscript in L440-442:

198 *The anomalously high AOD over the Southern Ocean in January 2020 reaches*
199 *values of up to 0.5 in some regions, consistent with independent data sources (e.g.,*
200 *MODIS AOD, see Supplement).*



201

202 **Fig. R3-1. Global AOD for January 2020 at 550 nm from MODIS/Aqua Level 3 product.**

203 (3) We agree that the sharp zonal contrast of SSA along the orbit is closely related to
204 viewing geometry effects. In the revised analysis, we further examined the impact
205 of ocean glint geometry. When the glint angle is small ($\leq 40^\circ$), enhanced surface
206 reflection over ocean increases the sensitivity of the retrieval to geometry-related
207 biases. After excluding oceanic pixels with glint angle $\leq 40^\circ$, the sharp contrast of
208 SSA along the orbit is substantially reduced, and the spatial continuity of the
209 retrievals is significantly improved. This improvement confirms that the previously
210 observed discontinuities are indeed strongly associated with viewing geometry
211 effects. We have updated the global maps, removed the previous statements
212 regarding zonal discontinuities, and added a detailed description of the pixel-
213 screening procedure in the revised manuscript in L198:

214 *Pixels with glint angle $\leq 40^\circ$ over ocean are also excluded, because enhanced*
215 *specular reflection at small glint angles reduces the aerosol information content*
216 *and may introduce geometry-dependent artifacts.*

217 **Specific comments:**

- 218 1. Line 44: It is somewhat misleading to claim that DPC follows up the data gap after
219 the retirement of the POLDER sensors because there are no Chinese investments
220 in international public data dissemination to my knowledge. If there is any news
221 about this, please comment or refer to an article. This is important for the European
222 community that is the main target of this journal.

223 Thanks for reminding. We have revised the expression in the manuscript in L41:

224 *After the retirement of POLDER in 2013, operational spaceborne multi-angle*
225 *polarimetric observations became limited. The launch of the Directional*
226 *Polarimetric Camera (DPC) onboard Gaofen-5 in 2018 introduced a new source*
227 *of multi-angle polarimetric measurements. These observations have supported*
228 *developments in SSA retrievals in recent years.*

- 229 2. Line 76: “theoretical correction errors”. This expression is confusing. Is this the
230 magnitude of correction, or the remaining bias after applying the correction? Please
231 clarify.

232 We are sorry for the confusion. What we intend to convey is that this uncertainty originates
233 from the calibration method itself, which are related to uncertainties of input parameters.
234 We have revised the expression in the manuscript in L87:

235 *The uncertainty associated with the calibration method is about 1-7 % (depending*
236 *on the wavelength and VZA).*

- 237 3. Lines 84-86: “Considering relatively ...”. Two referenced papers are not providing
238 the ground to use a single aerosol model to analyze polarimetric measurements.
239 Both studies focused on MODIS retrievals.

240 We are sorry for the confusion. We agree that the two cited studies focused on MODIS
241 scalar retrievals and therefore do not directly justify the use of a single aerosol model for
242 polarimetric measurements. In both studies, sensitivity experiments were conducted by
243 employing different aerosol models, and the results indicated that retrieval errors induced
244 by the phase matrix were smaller than those associated with AOD, SSA, and surface albedo.

245 However, these analyses were based on single-angle scalar observations rather than
246 polarization measurements. To address this concern more rigorously in the present study,
247 we have added additional sensitivity experiments to explicitly evaluate the impact of the
248 aerosol phase matrix within our retrieval framework. The results confirm that, although
249 some variability is introduced by different phase matrices, the induced uncertainties remain
250 smaller than those associated with other parameters. The corresponding analyses and
251 discussions have been incorporated into the revised manuscript in Sect. 3.1 to provide a
252 more solid justification for the adopted aerosol model configuration.

253 4. Lines 121-122: “accurately”, “high-precision”. The relevance to this paper is the
254 accuracy and precision needed for this research. Unless there are strict requirements
255 that limits the choice of radiative transfer models, I suggest removing these non-
256 quantitative expressions.

257 We thank the reviewer for the suggestion. We agree that the terms “accurately” and “high-
258 precision” are qualitative and not strictly quantified in this context. Since this study does
259 not impose explicit accuracy or precision constraints that would limit the choice of
260 radiative transfer models, these expressions have been removed to avoid overstatement.
261 We have revised the expression in L135-137 to focus on the functional capabilities of the
262 model rather than qualitative performance descriptions:

263 *It simulates Stokes vectors and their linearized matrices (Jacobians) at arbitrary*
264 *altitudes and viewing geometries, providing radiative simulations for satellite*
265 *remote sensing applications and serving as an effective forward model in numerical*
266 *inversion algorithms (Spurr, 2006).*

267 5. Line 157: “fixed constants”. Optimal estimation is a blending of a priori and
268 measurements, and therefore the assumption used in the a priori can easily bias the
269 estimation when the measurement information content is not sufficient. The precise
270 values used in this study should be presented with reasons of choice.

271 We thank the reviewer for the insightful comment. We agree that, in general, the choice of
272 a priori assumptions in optimal estimation may influence the retrieval when the
273 measurement information content is limited. In this study, however, the focus is on

274 evaluating the robustness and reliability of the retrieval algorithm itself under a controlled
275 and simplified configuration. Therefore, fixed a priori values and associated errors are
276 adopted to ensure consistency and reproducibility of the results. The a priori values and
277 associated errors for AOD and SSA are derived from the mean and standard deviation of
278 AERONET observations, providing physically reasonable and observationally based
279 constraints. The a priori estimates of surface properties are also prescribed as fixed values,
280 with their associated uncertainties defined according to the corresponding ranges of
281 variability. These a priori values and associated errors have been documented in Table 3 in
282 the manuscript, and a corresponding description has been added in L189-194:

283 *For AOD and SSA, the a priori state vector and its associated error covariance*
284 *matrix are prescribed as fixed values, derived from the mean and variance of*
285 *AERONET measurements. The a priori estimates of surface properties are also*
286 *fixed, with their errors defined by the corresponding ranges of variability. The use*
287 *of fixed a priori values is intended to provide a controlled and consistent*
288 *configuration for evaluating the inherent performance of the retrieval algorithm.*
289 *Details of the a priori values and associated errors are summarized in Table 3.*

290 6. Line 211: This section presents the results of numerical simulation, but the
291 simulation geometry is not mentioned anywhere, limiting the reproducibility of the
292 obtained results.

293 We thank the reviewer for pointing out this missing description. We agree that a clear
294 description of the simulation geometry is essential for the reproducibility of the sensitivity
295 experiments. In the revised manuscript, we have listed the SZA, VZA, and RAA in Table
296 4 used in the simulations. We have also added details in the manuscript in L216:

297 *The simulations were conducted under a series of SZA, VZA, and RAA, as listed in*
298 *Table 4.*

299 7. Lines 215-216: “not sensitive”. This sentence is an overstatement as only one
300 aerosol model and two land surface models are employed. It also contradicts to the
301 previous studies, notably to the study of critical surface albedo by Seidel and Popp
302 (2012).

303 We thank the reviewer for this important comment. We agree that the term “not sensitive”
304 was inappropriate and could be misleading in this context. The intended meaning of the
305 original statement was not that the magnitude of the response is insensitive to surface
306 parameters, but rather that, for the two land surface models considered, the response
307 patterns of ΔI and $\Delta DOLP$ to prescribed SSA perturbations are similar. We have revised
308 the text accordingly to emphasize the similarity in the overall trends, while explicitly
309 acknowledging the presence of differences in magnitude and angular distribution. We have
310 revised the expression in the manuscript in L253-255:

311 *Despite minor differences in magnitude and angular distribution, the changes in I*
312 *and DOLP induced by the prescribed SSA perturbations exhibit similar overall*
313 *patterns for the two land surface models considered.*

314 The revised expression avoids overgeneralization and does not imply a general insensitivity
315 to surface properties.

316 8. Figure 2, 3, and 4: Fluctuating results from the radiative transfer simulation of such
317 smooth phase function is surprising. Are small fluctuations of these curves
318 significant? What is the precision of the radiative transfer simulation in this study?
319 Adding error bound and explanation in the main text deems necessary.

320 Thank you for this constructive comment. The scattering angle is calculated from various
321 combinations of SZA, VZA, and RAA, which are grouped into bins and are now listed in
322 Table 4 in the revised manuscript. For similar scattering angles, the corresponding SZA-
323 VZA-RAA combinations may differ substantially. Such differences may lead to distinct
324 atmospheric photon path lengths in the radiative transfer calculations. In addition, the
325 surface reflectance is also anisotropic, which may also attribute to variations in simulated
326 TOA radiance. To further clarify this issue, we have provided the error bounds in the
327 updated figures. The error bounds are now explicitly reported in the manuscript.

328 9. Line 251: In this section (Section 3.2) and in the following section (Section 3.3), I
329 consider that it is necessary to perform the performance comparison at 550 nm (or
330 565 nm) rather than at 443 nm. Otherwise, this manuscript is not comparable to
331 other previous publications that authors themselves referenced. As authors mention

332 near Line 285, the retrieval performance depends on wavelength and available
333 information. This is why the comparison at an inconsistent wavelength is not
334 adequate.

335 We thank the reviewer for this important comment. In the revised manuscript, we have
336 added the corresponding analysis at 565 nm in Sects. 3.2 and 3.3. This ensures better
337 comparability with prior publications and provides a more appropriate evaluation of the
338 retrieval performance across wavelengths.

339 10. Line 254: “443 nm AOD”. This has to be kept as AOT at 443 nm, even when
340 comparing the performance of AOT and SSA at 550 nm, in order to be consistent
341 with AERONET processing algorithm that applies the “fine mode filter” by AOT
342 440 nm.

343 We thank the reviewer for pointing it out. We have revised the text to explicitly state that
344 the fine-mode filtering is consistently based on AOD at 443 nm, in line with the AERONET
345 processing algorithm that applies the filter at 440 nm. This AOD (443 nm) threshold is
346 used solely as a selection criterion for SSA validation and is applied uniformly throughout
347 the analysis, independent of the wavelength at which AOD or SSA performance is
348 evaluated. The expression in the manuscript has been revised in L295-298:

349 *For this reason, the validation applied an AOD-based screening criterion using*
350 *AOD_{443} (AOD at 443 nm). Only SSA retrievals with $AOD_{443} > 0.4$ were retained,*
351 *consistent with the AERONET fine-mode filtering criterion. This criterion was*
352 *applied uniformly throughout the analysis, independent of the wavelength at which*
353 *AOD or SSA was evaluated.*

354 11. Line 288: Same comment as Line 251 for this section.

355 Thanks for the comment. As mentioned above, analysis at 565 nm has also been added in
356 Sect. 3.3.

357 12. Line 292: “similar performance”. This reads contradictory to Line 266, “relatively
358 weaker performance”. The correlation coefficient of SSA drops from 0.688 at 443

359 nm to 0.347 at 565 nm, and it is difficult to claim that the performance at 565 nm
360 is “similar” to that at 443 nm.

361 We are sorry for the confusion. We agree that the phrase “similar performance” was
362 inappropriate and could be misleading, given the clear degradation in SSA retrieval
363 performance from 443 nm to 565 nm. The intended meaning was that the wavelength
364 dependence of the retrieval performance, namely the decreasing performance with
365 increasing wavelength, is consistent with the behavior observed in the simulated-data
366 experiments. However, in the revised manuscript, we have updated the retrieval experiment,
367 and the expression about “similar performance” has been removed.

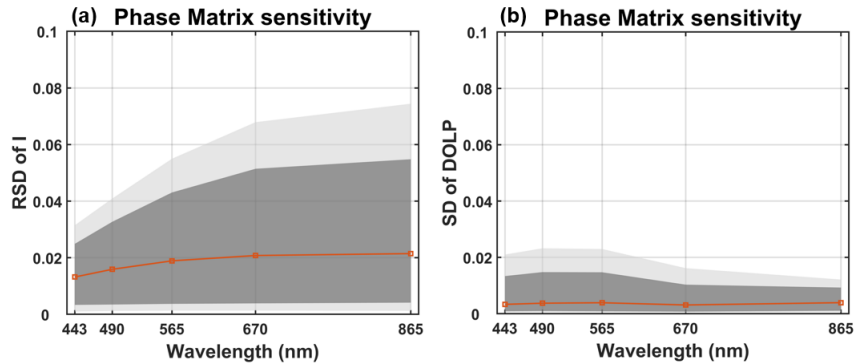
368 13. Line 299: “comparable to the operational MODIS AOD product (Levy et al.,
369 2010)”. This claim is an overstatement. The referenced paper reports the correlation
370 coefficient of 0.896 for AOT at 470 nm and 0.882 for AOT at 550 nm. This sentence
371 claims that correlation coefficient of 0.75 for AOT at 443 nm is comparable.

372 We thank the reviewer for this comment. We agree that the correlation coefficient of 0.75
373 obtained in this study is lower than those reported for the operational MODIS AOD product
374 in Levy et al. (2010), and the original expression was therefore an overstatement. The text
375 has been revised in L334-336 to acknowledge that the performance is weaker than that of
376 the operational MODIS product, while still indicating that the retrieved AOD shows a
377 reasonable level of consistency with AERONET observations:

378 *This performance is slightly lower than that reported for the operational MODIS*
379 *AOD products (Levy et al., 2010), but it is comparable in terms of AOD correlation*
380 *to the DPC retrievals reported by Dong et al. (2024), who obtained a correlation*
381 *coefficient of 0.76 for AOD at 670 nm.*

382 14. Line 339: “strong absorption properties”. In Levy et al. 2007a, heavy smoke by
383 biomass burning is recommended to be modeled by their “absorbing” model,
384 instead of “moderately absorbing” model, while this study uses their “moderately
385 absorbing” model and employ the heavy smoke case as a case study. It is worth
386 mentioning the reasons behind the inconsistency.

387 Thank you for this insightful comment. To address this concern, we conducted additional
 388 sensitivity experiments in Sect. 3.1 to quantify the impact of using different phase matrices
 389 on the retrieval results. We also present the results in Fig. R3-2. The analysis shows that
 390 the errors introduced by the choice of phase matrix are relatively small. Therefore, the use
 391 of the “moderately absorbing” model does not lead to significant biases in the heavy smoke
 392 case considered in this study.



393

394 **Fig. R3-2. Relative standard deviation (RSD) of I (a) and standard deviation (SD) of DOLP (b)**
 395 **induced by variations in phase matrix.**

396 **Technical comments:**

- 397 1. Line 67: “normalized radiation”. normalized radiance

398 Thanks for reminding. We have revised the expression in the manuscript.

- 399 2. Lines 140-141, 145: x_a . Using x_a as a-posteriori state vector is rather confusing as
 400 S_a is used for a-priori variance-covariance matrix. I suggest replacing by \hat{x} (x-hat,
 401 circumflex above x), following the common convention.

402 Thanks for the suggestion. We have replaced \mathbf{x}^a with $\hat{\mathbf{x}}$ in the manuscript.

403 **Reference**

404 Dong, Y., Li, J., Zhang, Z., Zheng, Y., Zhang, C., & Li, Z. (2024). Machine learning-based
 405 retrieval of aerosol and surface properties over land from the gaofen-5 directional
 406 polarimetric camera measurements. *IEEE Transactions on Geoscience and Remote*
 407 *Sensing*, 62, 1–15. <https://doi.org/10.1109/tgrs.2024.3419169>

408 Levy, R. C., Remer, L. A., & Dubovik, O. (2007). Global aerosol optical properties and
409 application to moderate resolution imaging spectroradiometer aerosol retrieval over land.
410 *Journal of Geophysical Research: Atmospheres*, *112*(D13), D13210.
411 <https://doi.org/10.1029/2006jd007815>

412 Levy, R. C., Remer, L. A., Kleidman, R. G., Mattoo, S., Ichoku, C., Kahn, R., & Eck, T.
413 F. (2010). Global evaluation of the collection 5 MODIS dark-target aerosol products over
414 land. *Atmospheric Chemistry and Physics*, *10*(21), 10399–10420.
415 <https://doi.org/10.5194/acp-10-10399-2010>

416 Li, Z., Hou, W., Hong, J., Zheng, F., Luo, D., Wang, J., et al. (2018). Directional
417 polarimetric camera (DPC): Monitoring aerosol spectral optical properties over land from
418 satellite observation. *Journal of Quantitative Spectroscopy and Radiative Transfer*, *218*,
419 21–37. <https://doi.org/10.1016/j.jqsrt.2018.07.003>

420 Zhu, S., Li, Z., Qie, L., Xu, H., Ge, B., Xie, Y., et al. (2022). In-flight relative radiometric
421 calibration of a wide field of view directional polarimetric camera based on the rayleigh
422 scattering over ocean. *Remote Sensing*, *14*(5), 1211. <https://doi.org/10.3390/rs14051211>